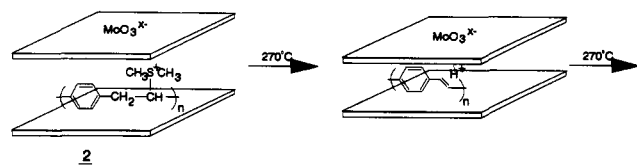


Scheme I



line shape. The spectrum was fit with three Gaussian peaks: B1 (78%) at 284.6 eV, B2 (16%) at 285.5 eV, and B3 (6%) at 287.1 eV. The first two bands are the same as those reported for pristine PPV.^{16,17} The band at 287.1 eV has been attributed to electron-deficient sites on the chain created when the polymer is p-doped. The spectrum is identical to that obtained for PPV lightly p-doped either by electrochemical oxidation or with AsF₅.^{16,17} We observed the same C_{1s} spectrum from 3 heat-treated in air, although in this case a fourth band was also visible at still higher binding energy (288.1 eV, 4% of the total intensity) which we ascribe to partial oxidation of the polymer chain.

Two (and four-probe) dc conductivity measurements on thin films of 3 revealed an increase in room-temperature conductivity (to ~0.5 S cm⁻¹) of more than 1 order of magnitude greater than the alkali molybdenum oxide, Na_{0.25}MoO₃, and 2 orders of magnitude greater than similarly treated monomer-intercalated MoO₃.^{10,18} Variable-temperature conductivity data show thermally activated charge-transport behavior characteristic of a semiconductor. Our data indicates that the increase in conductivity observed in the PPV-MoO₃ films does *not* arise from deoxygenation of the MoO₃ lattice.¹⁹

These data are consistent with the formation of p-doped PPV within the oxide layers. PPV is an insulator ($\sigma = 10^{-13}$ S cm⁻¹) and, hence, cannot directly increase the conductivity of the composite material. Conductivities for p-doped PPV films (e.g., with AsF₅), however, can exceed 10³ S cm⁻¹.^{1,3} We have proposed a series of events that may occur during the formation of PPV (Scheme I). Ion exchange, followed by mild heat treatment, initially forms [HPPV]_xMoO₃, in which the H⁺ is probably coordinated to the MoO₃ lattice, but could also interact with the conjugated PPV chain. If H_xMoO₃ were formed, it would convert to MoO₃ at 150 °C by the evolution of H₂ (air) or to MoO_{3-x/2} by the evolution of H₂O (vacuum, N₂).²⁰ This could not give rise to the observed conductivity: MoO₃ is an insulator, and we have determined the conductivity of substoichiometric MoO_{3-x/2} to be $\sigma = 10^{-5}$ S cm⁻¹ at room temperature. The proton could, however, oxidize the polymer chain by removal of an electron (hence forming a radical carbocation site on the PPV chain). This is analogous to p-doping PPV with H₂SO₄, which is known to produce a highly conductive form of the polymer.^{1,3}

We have shown that a new type of intercalation reaction is possible, in which high molecular weight ionomers can be inserted between the layers of inorganic oxides by ion exchange. This is distinguishable from an imbibition process.²¹ The ionomers enter the interlamellar gap as linear chain molecules to provide interleaved stacks of polymer/oxide which are well-ordered. This has yielded a novel nanocomposite of PPV and MoO₃ that is not obtainable by in situ polymerization.

Acknowledgment. We thank the NSERC for financial support and Drs. Brodie and Corbett of the physics department for use

(16) Obrzut, M. J.; Karasz, F. E. *Macromolecules* **1989**, *22*, 458.

(17) Masse, M. A.; Hirsch, J. A.; White, V. A.; Karasz, F. E. *New Polym. Mater.* **1990**, *2*, 75.

(18) The latter measurements were performed on thin films heat-treated under conditions identical to 3, except for the ionomer-intercalated MoO₃ which was heated at 50 °C.

(19) XPS measurements on thin films of 2, 3, and Na_xMoO₃ all showed an O/Mo ratio of close to 3, and Mo_{3d} high-resolution spectra showed no significant difference in the Mo(V)/Mo(VI) ratio. If deoxygenation was responsible for the increased conductivity, we would also have expected it to occur in monomer-intercalated MoO₃.

(20) Sotani, N.; Eda, K.; Kunitomo, M. *J. Chem. Soc., Faraday Trans.* **1990**, *86*, 1583 and references therein.

(21) Ruiz-Hitzky, E.; Aranda, P. *Adv. Mater.* **1990**, *2*, 545.

of their conductivity apparatus. We also thank Dr. S. McIntyre and Perry Spevak (Surface Science Western) for the XPS measurements.

Supplementary Material Available: XPS spectra, FT-IR spectra, X-ray diffraction patterns, and conductivity data for 1 and 2 (11 pages). Ordering information is given on any current masthead page.

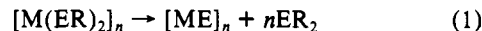
Synthesis of Reactive Homoleptic Tellurolates of Zirconium and Hafnium and Their Conversion to Terminal Tellurides: A Model for the First Step in a Molecule-to-Solid Transformation

Victor Christou and John Arnold*

Department of Chemistry, University of California Berkeley, California 94720

Received January 31, 1992

Compounds incorporating elements from groups 12 and 16 (so-called II-VI materials) are increasingly important due to their remarkable electronic properties.¹⁻¹³ The use of molecular species as precursors to these materials is particularly appealing,¹⁴ since the products may be prepared in a variety of forms, including nanoclusters, thin films, and bulk solids; however, little is known of the pathway involved in the molecule-to-solid transformation.¹⁵ The metal chalcogenolate starting materials are known to decompose to chalcogenides as in eq 1 (where M = Zn, Cd, Hg; E = S, Se, Te; and R = aryl, alkyl).



We sought to monitor the progress of elimination reactions of this general type by using well-defined soluble model compounds. Here we report studies of homoleptic tellurolate derivatives of early transition metals where preliminary evidence suggests that these complexes undergo similar elimination reactions in the solid state. Analogous reactivity is also observed in homogeneous solution; in this case, however, we have been able to isolate and fully characterize the presumed M=Te intermediates. This chalcogenolate-to-chalcogenide transformation may be viewed as a homogeneous model for the first step in the thermal decomposition of a molecular compound to a solid-state material.

Using the synthetically versatile, sterically demanding ⁻TeSi-(SiMe₃)₃ ("sitel") ligand, we prepared the brightly colored hom-

(1) Steigerwald, M. L.; Sprinkle, C. R. *J. Am. Chem. Soc.* **1987**, *109*, 7200.

(2) Alivisatos, A. P.; Harris, T. D.; Carroll, P. J.; Steigerwald, M. L.; Brus, L. E. *J. Chem. Phys.* **1989**, *90*, 3463.

(3) Cummins, C. C.; Beachy, M. D.; Schrock, R. R.; Vale, M. G.; Sankaran, V.; Cohen, R. E. *Chem. Mater.* **1991**, *3*, 1153.

(4) Osakada, K.; Yamamoto, T. *J. Chem. Soc., Chem. Commun.* **1987**, 1117.

(5) Brennan, J. G.; Siegrist, T.; Carroll, P. J.; Stuczynski, S. M.; Brus, L. E.; Steigerwald, M. L. *J. Am. Chem. Soc.* **1989**, *111*, 4141.

(6) Brennan, J. G.; Siegrist, T.; Carroll, P. J.; Stuczynski, S. M.; Reyniers, P.; Brus, L. E.; Steigerwald, M. L. *Chem. Mater.* **1990**, *2*, 403.

(7) Dameron, C. T.; Reese, R. N.; Mehra, R. K.; Kortan, A. R.; Carroll, P. J.; Steigerwald, M. L.; Brus, L. E.; Winge, D. R. *Nature (London)* **1989**, *338*, 596.

(8) Steigerwald, M. L.; Sprinkle, C. R. *Organometallics* **1988**, *7*, 245.

(9) Steigerwald, M. L.; Brus, L. E. *Annu. Rev. Mater. Sci.* **1989**, *19*, 471.

(10) Steigerwald, M. L.; Brus, L. E. *Acc. Chem. Res.* **1990**, *23*, 183.

(11) Kortan, A. R.; Hull, R.; Opila, R. L.; Bawendi, M. G.; Steigerwald, M. L.; Carroll, P. J.; Brus, L. E. *J. Am. Chem. Soc.* **1990**, *112*, 1327.

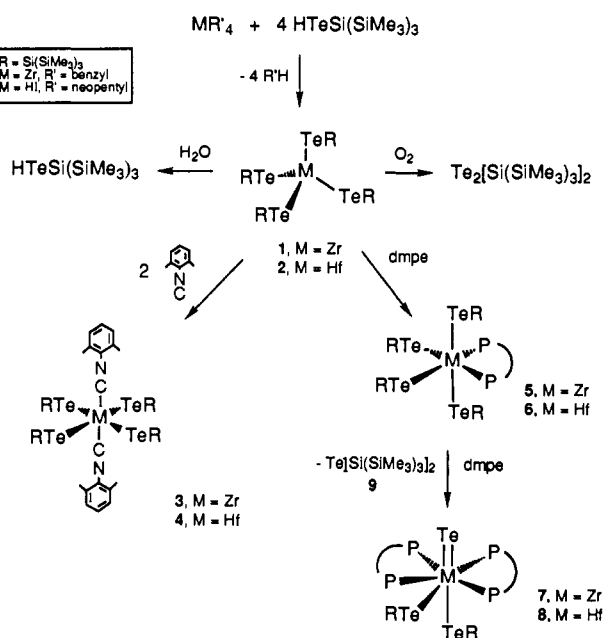
(12) Bochmann, M.; Webb, K. J.; Hursthouse, M. B.; Mazid, M. *J. Chem. Soc., Dalton Trans.* **1991**, 2317.

(13) Bochmann, M.; Webb, K. J. *J. Chem. Soc., Dalton Trans.* **1991**, 2325.

(14) O'Brien, P. *Chemtronics* **1991**, *5*, 61.

(15) Steigerwald, M. L.; Siegrist, T.; Stuczynski, S. M. *Inorg. Chem.* **1991**, *30*, 4940.

Scheme 1



oleptic tellurolates of Zr (**1**, green) and Hf (**2**, red) via tellurololysis^{16–18} of the metal tetraalkyls as shown in Scheme 1.¹⁹ No byproducts were detected in these reactions, and isolated yields of analytically pure material ranged from 70 to 85% after recrystallization from concentrated hexane.²⁰ As with the group 1 derivatives, the compounds react cleanly with water and dry oxygen to give the tellurol and ditelluride $Te_2[Si(SiMe_3)_3]_2$,¹⁶ respectively. They are thermally stable, high-melting solids that show intense signals for the molecular ion by EI/MS. Singlets due to the sited ligand were observed in the ¹H, ¹³C{¹H}, and ¹²⁵Te{¹H} NMR spectra of both compounds.

The X-ray crystal structures of both **1** and **2** have been determined;²¹ these are the first reports of crystallographically characterized early transition metal tellurolates. The structure of **1** consists of well-separated molecules with the zirconium surrounded by four tellurium atoms in a pseudotetrahedral array.²² The Te–Zr–Te angles vary across a wide range from 101.63 (2)° up to 115.89 (2)°, presumably due to interligand repulsions from the bulky sited. The Zr–Te bond lengths (2.724 (1)–2.751 (1) Å) are in the range predicted on the basis of ionic radii (2.80 Å).²³

These sterically encumbered compounds react readily with a wide variety of Lewis bases to form, in the case of 2,6-xylyl isocyanide, the six-coordinate trans species **3** and **4**. Addition of excess isocyanide produces the disilytelluride **9** and an intractable, hexane-soluble brown oil. One equivalent of the chelating phosphine dmpe [1,2-bis(dimethylphosphino)ethane] forms related cis adducts (**5** and **6**) that were characterized by ¹H, ¹³C{¹H}, ³¹P{¹H}, and ¹²⁵Te{¹H} NMR spectroscopy. In these cases, however, reaction with an additional 1 equiv of dmpe results in a clean transformation to produce 1 equiv of **9** and the seven-coordinate metal telluride complexes **7** and **8**. These reactions are quantitative as monitored by ¹H NMR spectroscopy, and isolated yields are typically between 50 and 80%. Terminal metal tellurides are

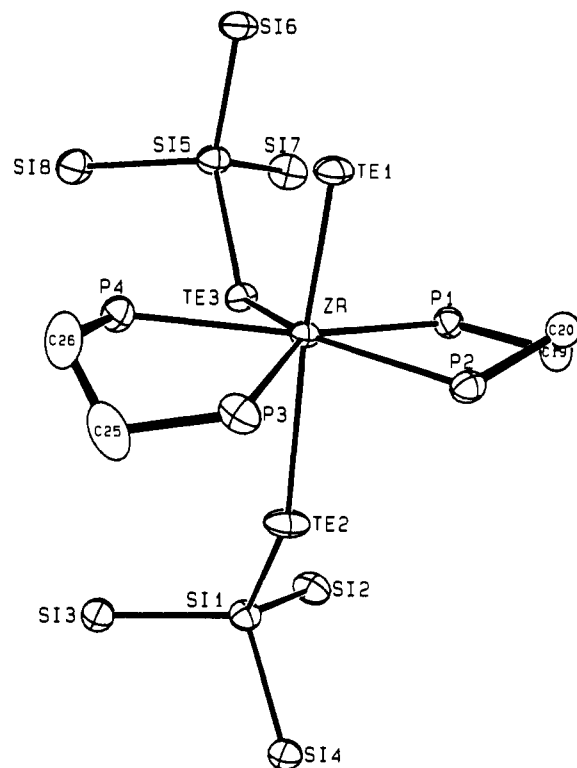


Figure 1. ORTEP view of $ZrTe[TeSi(SiMe_3)_3]_2(dmpe)_2$ with thermal ellipsoids at 50% probability. Methyl groups are omitted for clarity.

extremely rare; the only other example is the recently reported 18-electron species $W(PMe_3)_4(Te)_2$.²⁴

The metal tellurides are deep red-brown, highly air-sensitive crystalline materials. Both show evidence for stereochemical nonrigidity in toluene at room temperature by NMR spectroscopy.²⁰ Variable temperature studies showed that the proton and phosphorus signals sharpen at –85 °C, and when the temperature was raised above 40 °C, the sited proton resonances, which are broad at 20 °C, coalesced to a singlet. At –85 °C, the ¹²⁵Te{¹H} NMR spectrum of **7** shows three signals at δ –706, –1173, and –1197 ppm. We assign the upfield signals to the two inequivalent sited ligands on the basis of (a) their remarkably similar chemical shifts and (b) the fact that the peak at –1173 ppm is split into a triplet (²J_{TeP} = 166 Hz) by two equivalent transoid phosphorus atoms, an arrangement confirmed by X-ray crystallography (see below). The low-field signal at δ –706 ppm is then assigned to the terminal telluride. This value is significantly upfield of that reported for $W(PMe_3)_4(Te)_2$ (δ +958),²⁴ but note that shift differences of this magnitude are not uncommon in ¹²⁵Te NMR spectroscopy.^{25–27}

The X-ray structures of both telluride species show the central metal atom coordinated in a roughly pentagonal bipyramidal fashion, comprising two dmpe ligands and one sited in the equatorial plane, with the terminal telluride and the remaining sited axial (Figure 1).²² The presence of two different Zr–Te interactions allows for comparison of tellurolate and telluride ligation in the same molecule. The Zr–TeSi(SiMe₃)₃ bond distances (2.939 (1) and 3.028 (1) Å for axial and equatorial siteds, respectively) are considerably longer than those found in the homoleptic complex, which range from 2.724 (1) to 2.751 (1) Å. By comparison, the Zr=Te interaction is much shorter at 2.650 (1) Å. This value is slightly longer than the W=Te distance of 2.596 (1) Å found in $W(PMe_3)_4(Te)_2$,²⁴ however, after consideration of effective ionic radii (seven-coordinate Zr⁴⁺, 0.92 Å; six-coordinate W⁴⁺, 0.80

(16) Dabbousi, B. O.; Bonasia, P. J.; Arnold, J. J. *J. Am. Chem. Soc.* **1991**, *113*, 3186.

(17) Bonasia, P. J.; Gindelberger, D. E.; Dabbousi, B. O.; Arnold, J. J. *Am. Chem. Soc.*, in press.

(18) Bonasia, P. J.; Arnold, J. J. *Chem. Soc., Chem. Commun.* **1990**, 1299.

(19) All reactions in Scheme 1 were carried out at 20 °C in hexane.

(20) Full characterization data are provided as supplementary material.

(21) Details of the crystallographic characterization of **1** and **7** and an ORTEP view of **1** are provided as supplementary material.

(22) The hafnium derivatives are isostructural with almost identical metrical parameters; these data will be presented later.

(23) Shannon, R. D.; Prewitt, C. T. *Acta Crystallogr.* **1969**, *B25*, 925. Shannon, R. D. *Acta Crystallogr.* **1976**, *A32*, 751.

(24) Rabinovich, D.; Parkin, G. *J. Am. Chem. Soc.* **1991**, *113*, 9421.

(25) McFarlane, H. C. E.; McFarlane, W. In *Multinuclear NMR*; Mason, J., Ed.; Plenum: New York, 1987; p 417.

(26) Fazakerley, G. V.; Celotti, M. J. *Magn. Reson.* **1979**, *33*, 219.

(27) Zumbulyadis, N.; Gysling, H. J. *J. Organomet. Chem.* **1980**, *192*, 183.

Å),²³ the difference is hardly significant.

Preliminary studies show that solid-state thermolysis of **1** from 200 to 375 °C under vacuum results in the formation of a mixture of volatile products containing **9**, Me₃SiTeSi(SiMe₃)₃,¹⁷ and other uncharacterized SiMe₃-containing products (by ¹H NMR spectroscopy), along with a black powder containing zirconium telluride.²⁸ Further details regarding these reactions, and those in other related complexes, will be presented in a full account.

Acknowledgment. We thank the National Science Foundation (CHE-9019675) for financial support.

Registry No. **1**, 141784-70-5; **2**, 141784-71-6; **3**, 141784-64-7; **4**, 141784-65-8; **5**, 141784-66-9; **6**, 141784-67-0; **7**, 141784-68-1; **8**, 141784-69-2; **9**, 141784-63-6; HTeSi(SiMe₃)₃, 133100-98-8; Zr(CH₂Ph)₄, 24356-01-2; Hf(*neo*-C₅H₁₁)₄, 50654-35-8; 2,6-dimethylisocyanobenzene, 2769-71-3.

Supplementary Material Available: Details of structure determinations including tables of crystal and data collection parameters, temperature factor expressions, positional parameters, intramolecular distances and angles, and least-squares planes for **1** and **7** (31 pages); listing of observed and calculated structure factors for **1** and **7** (124 pages). Ordering information is given on any current masthead page.

(28) Elemental analysis showed the powder to contain low levels of carbon and hydrogen (1.4% and 0.4%, respectively). X-ray powder diffraction indicated the presence of ZrTe₃. Further studies are in progress.

Preparation of Stable Magnesium, Calcium, Strontium, and Barium Tellurolates and the X-ray Crystal Structures of Mg[TeSi(SiMe₃)₃]₂(THF)₂ and Ca[TeSi(SiMe₃)₃]₂(THF)₄

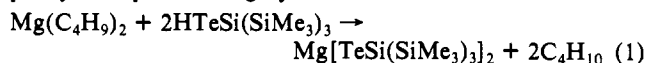
David E. Gindelberger and John Arnold*

Department of Chemistry, University of California
Berkeley, California 94720
Received February 10, 1992

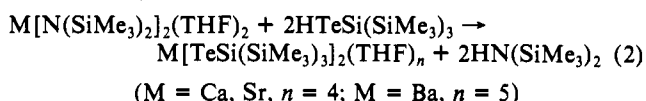
It is well known that tellurium inserts into reactive magnesium-carbon bonds of aryl Grignards to form solutions containing tellurolate (TeR) species.¹⁻⁵ Although reactivity studies have shown these compounds to be useful reagents in organotellurium chemistry, their apparent instability has prohibited their isolation and characterization; as a result, little is known regarding their structures and properties. Tellurolate derivatives of calcium, strontium, or barium are, to the best of our knowledge, unknown. Recently we reported some remarkably stable alkali metal tellurolate derivatives based on the sterically hindered TeSi(SiMe₃)₃ ("sitel") ligand, together with preliminary studies of their synthetic potential.^{6,7} Here we describe an extension of this chemistry leading to the first isolable, well-characterized examples of group 2 tellurolates.

Methods relying on direct insertion of tellurium into metal-Si(SiMe₃)₃ bonds could not be tested as the necessary starting materials are unknown, and metathesis reactions between the lithium tellurolate (THF)₂LiTeSi(SiMe₃)₃ and group 2 dihalides led only to intractable mixtures. In contrast, tellurolate reactions⁶ involving metal-nitrogen or metal-carbon bonds afforded an extremely clean and simple route to the metal tellurolates. For

example, eq 1 shows the tellurolate of dibutylmagnesium in hexane, which gave the base-free, homoleptic sitel compound as pale yellow plates in high yield.



The structure of this derivative is presently unknown; however, a bis-THF adduct, prepared by recrystallization in the presence of THF, has been characterized by X-ray crystallography (see below). Reactions between the well-defined, hydrocarbon-soluble group 2 silylamides⁸ and 2 equiv of HTeSi(SiMe₃)₃⁶ in hexane gave high yields of the corresponding sitel complexes of calcium, strontium, and barium, which were isolated and crystallized as THF adducts.⁹

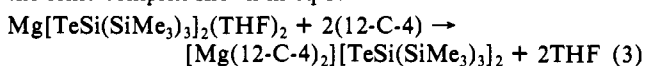


At room temperature, the THF complexes slowly lose coordinated solvent, but they are otherwise stable to heat and normal room light and can be kept under nitrogen for prolonged periods of time. The analogous pyridine adducts were readily prepared by recrystallization of the THF complexes from pyridine.

The group 2 tellurolate adducts are highly crystalline, pale yellow, air-sensitive materials with high melting points. Dissolution in hydrocarbon and ethereal solvents affords concentrated solutions that are stable indefinitely in the absence of O₂ and water. As with the group 1 derivatives, the group 2 compounds react cleanly with water and dry oxygen to give the tellurol and ditellurol Te₂[Si(SiMe₃)₃]₂, respectively.⁶ For the series of pyridine adducts, ¹²⁵Te NMR spectra show singlets in the range -1405 to -1578 ppm (relative to Me₂Te at 0 ppm). Although these values occur at significantly higher field than alkyl- and aryltellurolate derivatives,¹⁰ they are typical of salts incorporating the sitel ligand (cf. the lithium derivative [(THF)₂LiTeSi(SiMe₃)₃]₂ δ -1622).^{7a}

In contrast to the metal amide starting materials, which are all four coordinate, the sitel complexes crystallize with varying numbers of donor ligands as determined by ¹H NMR spectroscopy and elemental analyses. In the case of pyridine, for example, Mg²⁺ (effective ionic radius 0.71 Å)¹¹ forms a four-coordinate species, whereas the larger Ba²⁺ ion (1.52 Å) accommodates a structure with five donor ligands.

Treatment of the magnesium derivative with 12-crown-4 results in displacement of both the THF and the sitel ligands to form the ionic complex shown in eq 3:



Crystals of the 2:1 salt (Δ_M = 200 cm² Ω⁻¹ mol⁻¹, 0.1 M MeCN)¹² were isolated as pale yellow plates from THF. At 20 °C, the

(8) Bradley, D. C.; Hursthouse, M. B.; Ibrahim, A. A.; Malik, K. M. A.; Motevalli, M.; Mösele, R.; Powell, H.; Runnacles, J. D.; Sullivan, A. C. *Polyhedron* 1990, 9, 2959.

(9) Selected characterization data: Mg(sitel)₂ ¹H NMR (400 MHz, C₆D₆) δ 0.44 (s); Mg(sitel)₂(THF)₂ ¹H NMR (400 MHz, C₆D₆) δ 3.79 (m, 8 H), 1.23 (m, 8 H), 0.50 (s, 54 H); Mg(sitel)₂(pyr)₂ ¹H NMR (300 MHz, C₆D₆) δ 8.86 (d, 4 H), 6.79 (t, 2 H), 6.52 (t, 4 H), 0.45 (s, 54 H), ¹²⁵Te[¹H] NMR (157.7 MHz, C₆D₆) δ -1578; Mg[12-crown-4]₂[TeSi(SiMe₃)₃]₂ ¹H NMR (400 MHz, CD₃CN) δ 3.92 (m, 32 H), 0.13 (s, 54 H); Ca(sitel)₂(THF)₄ ¹H NMR (400 MHz, C₆D₆) δ 3.79 (m, 16 H), 1.47 (m, 16 H), 0.48 (s, 54 H); Cs(sitel)₂(pyr)₄ ¹H NMR (400 MHz, C₆D₆) δ 9.51 (d, 8 H), 6.82 (t, 4 H), 6.67 (t, 8 H), 0.42 (s, 54 H), ¹²⁵Te[¹H] NMR (157.7 MHz, C₆D₆) δ -1458; Sr(sitel)₂(THF)₄ ¹H NMR (400 MHz, C₆D₆) δ 3.83 (m, 16 H), 1.54 (m, 8 H), 0.48 (s, 54 H); Sr(sitel)₂(pyr)₄ ¹H NMR (300 MHz, C₆D₆) δ 9.35 (d, 8 H), 6.80 (t, 4 H), 6.64 (t, 8 H), 0.48 (s, 54 H), ¹²⁵Te[¹H] NMR (157.7 MHz, C₆D₆) δ -1482 (s); Ba(sitel)₂(THF)₄ ¹H NMR (400 MHz, C₆D₆) δ 3.73 (m, 16 H), 1.48 (m, 16 H), 0.52 (s, 54 H); Ba(sitel)₂(pyr)₅ ¹H NMR (400 MHz, C₆D₆) δ 9.14 (d, 10 H), 6.82 (t, 5 H), 6.66 (t, 10 H), 0.52 (s, 54 H), ¹²⁵Te[¹H] NMR (157.7 MHz, C₆D₆) δ -1405 (s). Satisfactory elemental analyses were determined for all compounds except the THF adducts of Mg, Sr, and Ba, which lose coordinated solvent on drying.

(10) Bildstein, B.; Irgolic, K. J.; O'Brien, D. H. *Phosphorus Sulfur Relat. Elem.* 1988, 38, 245.

(11) Shannon, R. D.; Prewitt, C. T. *Acta Crystallogr.* 1969, B25, 925. Shannon, R. D. *Acta Crystallogr.* 1976, A32, 751.

(12) Geary, W. J. *Coord. Chem. Rev.* 1971, 7, 81.

(1) Irgolic, K. J. *The Organic Chemistry of Tellurium*; Gordon and Breach: New York, 1974.

(2) Gysling, H. J. In *The Chemistry of Organic Selenium and Tellurium Compounds*; Patai, S., Rappaport, Z., Eds.; Wiley: New York, 1986; Vol. 1, p 679.

(3) Petragnani, N.; de Moura Campos, M. *Chem. Ber.* 1963, 96, 249.

(4) Petragnani, N. *Chem. Ber.* 1963, 96, 247.

(5) Haller, W. S.; Irgolic, K. J. *J. Organomet. Chem.* 1972, 38, 97.

(6) Dabbousi, B. O.; Bonasia, P. J.; Arnold, J. *J. Am. Chem. Soc.* 1991, 113, 3186.

(7) (a) Bonasia, P. J.; Gindelberger, D. E.; Dabbousi, B. O.; Arnold, J. *J. Am. Chem. Soc.*, in press. (b) Bonasia, P. J.; Arnold, J. *Inorg. Chem.*, in press.